Floquet vortex states induced by light carrying an orbital angular momentum

Hwanmun Kim, Hossein Dehghani, Iman Ahmadabadi, Ivar Martin, and Mohammad Hafezi

Floquet vortex states induced by light carrying the orbital angular momentum

Hwanmun Kim,[1, 2] Hossein Dehghani,[1, 3] Iman Ahmadabadi,[1, 2] Ivar Martin,[4] and Mohammad Hafezi[1, 2, 3]

[1]*Joint Quantum Institute, NIST and University of Maryland, College Park, Maryland 20742, USA*
[2]*Department of Physics, University of Maryland, College Park, Maryland 20742, USA*
[3]*Departments of Electrical and Computer Engineering and Institute for Research in Electronics and Applied Physics,*
University of Maryland, College Park, Maryland 20742, USA
[4]*Materials Science Division, Argonne National Laboratory, Argonne, Illinois 60439, USA*
(Dated: January 6, 2022)

We propose a scheme to create an electronic Floquet vortex state by irradiating a two-dimensional semiconductor with the laser light carrying non-zero orbital angular momentum. We analytically and numerically study the properties of the Floquet vortex states, with the methods analogous to the ones previously applied to the analysis of superconducting vortex states. We show that such Floquet vortex states are similar to the superconducting vortex states, and they exhibit a wide range of tunability. To illustrate the potential utility of such tunability, we show how such states could be used for quantum state engineering.

I. INTRODUCTION

Quantum vortices and localized quantum states associated with them have long a subject of active interest in diverse areas of physics [1–6]. To create and observe such quantum vortex states, numerous efforts have been made in diverse systems such as Bose-Einstein condensates [7–12], superconductors [13, 14], and magnetic materials [15–17]. While the quantum vortex states themselves exhibit many exotic quantum and classical many-body phenomena [18–23], their stability as topological defects makes them a promising quantum platform for applications such as quantum information processing [24–26].

Recently, Floquet systems have become popular as a useful way to engineer exotic quantum states [27–37]. Moreover, there have been many recent advancements in the spatial control of optical beams in atomic systems [38–41]. These techniques have the potential to be applied to electronic systems and can provide a wide range of tunability in quantum state engineering.

In this paper, we present a scheme to create Flouqet quantum vortex states by shining a light field carrying orbital angular momentum (OAM) on a two-dimensional (2D) semiconductor, as illustrated in Fig.1. In small detuning and the weak field limit, we show that electronic Floquet vortex states are localized around the optical vortices with localization length bounded by the shape and intensity of the optical field. We also show that the number of vortex state branches is directly given by the vorticity of the light, which quantifies the OAM carried by each photon. Such close relation with OAM of light distinguish these vortex states from the edge states of the uniform Floquet Chern insulator [28] or the vortex states introduced in Ref. [30, 31]. While many characteristics of these Floquet vortex states carry close analogy with superconducting systems, we show that the Floquet vortex states in the current system benefit from a very broad range of tunability. For example, the freedom to choose the size of the optical vortex can be used as a knob to control the non-linearity of the vortex state
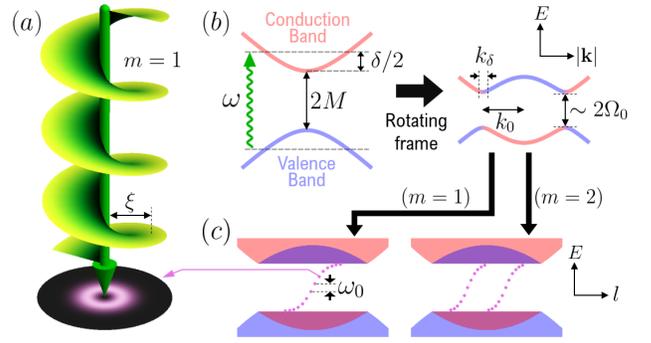
FIG. 1. (a) A 2D semiconductor illuminated by a laser light carrying OAM. The applied light field has the optical vortex structure of size ξ. The figure illustrates the case of vorticity $m = 1$. (b) The laser field has frequency ω, and couples the conduction and the valence bands of the semiconductor with the gap $2M$. The detuning is $\delta = \omega - 2M$. In the rotating frame, the hybridization gap of about $2\Omega_0$ develops around the resonance ring whose radius and thickness are k_0 and k_δ, respectively. (c) For the light field with non-zero vorticity m, $|m|$ branches of Floquet vortex states develop in the middle of the hybridization gap. Around the zero energy, each branch has linear dispersion with energy separation ω_0 between nearby states in the branch. Note that the energy spectrum is illustrated with respect to the electronic pseudo-OAM, l.

spectrum. To demonstrate how such tunability can be exploited for quantum state engineering, we construct a scheme of quantum information processing based on optically manipulating Floquet vortex states, with simple single-qubit and two-qubit operations.

II. MODEL

We consider $H_0 = (vk_x, vk_y, M) \cdot \sigma$ as our model for a spinless 2D semiconductor [42, 43]. For brevity, we have set $\hbar = 1$. Here, $\sigma = (\sigma_x, \sigma_y, \sigma_z)$ are Pauli

matrices. M is a half of the band gap and v is a parameter determining the curvature of the band dispersion $\pm\sqrt{M^2 + v^2(k_x^2 + k_y^2)}$, where the positive (negative) energy states correspond to the conduction (valence) band. We vertically shine a linearly-polarized laser field with a non-zero orbital angular momentum (OAM), $\mathcal{A}(\mathbf{r}, t) = A(\mathbf{r})e^{i\omega t}\hat{\mathbf{x}} + \text{c.c.}$ on a semiconductor, as illustrated in Fig. 1 where ω is the frequency of the laser field. The OAM of the laser field is represented in the azimuthal phase factor of $A(\mathbf{r}) = A_0(r)e^{im\phi}$, where $r = \sqrt{x^2 + y^2}$ and $\phi = \arctan(y/x)$. The integer m here is the vorticity of the field, and we refer the vortex structure with non-zero vorticity in the light field as an optical vortex. Due to this vortex structure, $A_0(r)$ should vanish at $r = 0$. We set the size of optical vortex to ξ, which means that $A_0(r)$ smoothly saturates to $A_{\max}$ at $r \geq \xi$. With the minimal coupling $\mathbf{k} = (k_x, k_y) \rightarrow \mathbf{k} + e\mathcal{A}(\mathbf{r}, t)$, we obtain the time-periodic Hamiltonian

$$H(t) = H_0 + ev\mathcal{A}(\mathbf{r}, t) \cdot \sigma. \tag{1}$$

When $\omega > 2M$, the frequency detuning $\delta = \omega - 2M$ becomes positive and the conduction and valence bands become resonant at the resonance ring of momentum, $|\mathbf{k}| = k_0 = v^{-1}\sqrt{\omega^2/4 - M^2}$. From Eq. (1), the applied laser field generates position-dependent Rabi frequency $\Omega(r) = evA_0(r)$ and hybridizes the conduction and valence bands while opening an energy gap about $2\Omega_0$ around the resonance ring, where $\Omega_0 = \lim_{r\to\infty} \Omega(r)$. To describe these hybridized bands, we consider the transformation into the rotating frame, $U(t) = P_c e^{-i\omega t/2} + P_v e^{i\omega t/2}$, where P_c (P_v) is the projection operator into the conduction (valence) band. In the weak field limit $\Omega_0 \ll \sqrt{\omega\delta}$, we can drop the fast oscillating terms from the rotated Hamiltonian $-iU^\dagger(t)\partial_t U(t) + U^\dagger(t)H(t)U(t)$ and obtain the effective Hamiltonian under the rotating wave approximation (RWA). Furthermore, we consider the small detuning regime $\delta \ll \omega$. In this regime, we can write $\delta \simeq v^2 k_0^2/M$ and $vk_0 \ll M$. Then, for the small momenta $|\mathbf{k}| = O(k_0)$ (see Supplemental Material),

$$H_{\text{RWA}} = \frac{\delta}{2}\left(\frac{\mathbf{k}^2}{k_0^2} - 1\right)\sigma_z + \left[\Omega(r)e^{-im\phi}\sigma_+ + \text{H.c.}\right], \tag{2}$$

where $\sigma_\pm = (\sigma_x \pm i\sigma_y)/2$.

III. FLOQUET VORTEX STATES

Because of the breaking of the translational symmetry by the optically-induced vortex, it is possible to have electronics states with energies inside the spectral gap that are localized in the vicinity of the vortex. From Eq. (2), we can estimate the spatial extent of such states. First, one can readily observe that the diagonal components are dominant over off-diagonal elements for most of $\mathbf{k}$s except the vicinity of the resonance ring. This means that the hybridization mostly occurs at the momenta in

the narrow region near the resonance ring, and the thickness of this region can be estimated by finding the range of $|\mathbf{k}|$ that makes the off-diagonal elements of Eq. (2) comparable to or larger than the diagonal elements. We find that the hybridization of the two bands occurs at $|\mathbf{k}| - k_0 = O(k_\delta)$ where $k_\delta \equiv k_0\Omega_0/\delta$, that characterizes the momentum range over which the Rabi frequency and dispersion of Eq.2 are comparable around the resonant momentum ring. If any intragap state develops within this hybridization gap, such a state should be a superposition of the Bloch states within this momentum region. Therefore k_δ^{-1} serves as a lower bound for the spatial size of such intragap state. If a localized intragap state develops around the optical vortex, this state cannot extend to the region where $A_0(r)$ saturates to $A_{\max}$ since the field is nearly uniform and therefore the system remains gapped. Therefore such a localized intragap state has an upper bound $O(k_\delta^{-1} + \xi)$ for its size.

By using the semiclassical argument introduced in Ref. [44], one can show that $|m|$ branches of intragap states develop around the optical vortex with vorticity m (see Supplemental Material). We call these states Floquet vortex states, and we can obtain a fully quantum-mechanical description of the dispersion and wavefunction of these states by applying mathematical methods used for superconducting vortices [45–48]. To do so, we note that while the effective Hamiltonian in Eq. (2) does not commute with the electronic OAM, $\hat{L} = -i\partial_\phi$, it does commute with the electronic pseudo-OAM, $\hat{l} = -i\partial_\phi + (m/2)\sigma_z$. Then the eigenstates of this effective Hamiltonian can be written in the form of vortex states,

$$\psi_{n,l}(\mathbf{r}) = \left(e^{i(l-m/2)\phi}u_{n,l,+}(r), e^{i(l+m/2)\phi}u_{n,l,-}(r)\right)^T. \tag{3}$$

Here, the branch index $n = 1, \cdots, m$ represents different branches of Floquet vortex states. One can also show that this system satisfies the particle-hole symmetry which requires $\psi_{n,-l}(\mathbf{r}) = i\sigma_y\psi_{|m|+1-n,l}^*(\mathbf{r})$ and $E_{n,-l} = -E_{|m|+1-n,l}$, where $E_{n,l}$ is the corresponding eigenenergy for $\psi_{n,l}(\mathbf{r})$. In the large optical vortex regime $k_\delta^{-1} \ll \xi$, the low-energy spectrum of these Floquet vortex states are given by [48]

$$E_{n,l} = ml\omega_0 + [n - (|m| + 1)/2]\tilde{\omega}_0, \text{ where}$$

$$\omega_0 = \frac{\delta \int_0^\infty \frac{\Omega(r)}{r} e^{-(2k_0/\delta)\int_0^r \Omega(r')dr'}dr}{k_0 \int_0^\infty e^{-(2k_0/\delta)\int_0^r \Omega(r')dr'}dr},$$

$$\tilde{\omega}_0 = \frac{\delta(\pi/2)}{k_0 \int_0^\infty e^{-(2k_0/\delta)\int_0^r \Omega(r')dr'}dr}. \tag{4}$$

Here, the energy separation between nearby states and branches, ω_0 and $\tilde{\omega}_0$, respectively, are solely determined by the bulk properties and the details of the radial beam profile $A_0(r)$. These parameters are independent of the system size and therefore the energy separation between states remains in the thermodynamic limit. This analytic expression of the dispersion is valid for the low-energy
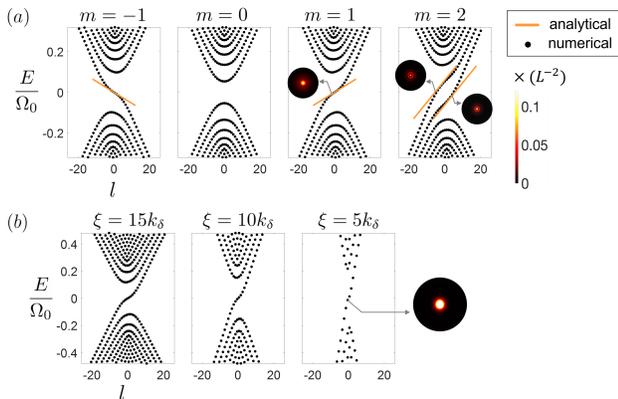
FIG. 2. (a) Numerically calculated energy spectra in terms of pseudo-OAM l. We use $\omega = 2.05M$, $A_{\max} = 0.09M(ev)^{-1}$, and $A_0(r) = A_{\max}\left[1 - \exp\{-r^2/(2\xi^2)\}\right]$, $\xi = 20k_\delta$, and suppose a disk sample of radius 25ξ. Note that we only exhibit spectra near the zero energy while the bulk gap is about $2\Omega_0$. The numerical spectra agree with the analytically expected dispersion in Eq. (4) including the number of intragap state branches and the slope of the linear dispersion for small $|E_l|$ and l. Electronic density profiles of selected states are presented in the insets. (b) Dispersions for $m = 1$ with identical parameters with (a) except the optical vortex size ξ and the disk size $500k_\delta$. As ξ reduces, the linear region of the spectrum shrinks while the energy separation between the nearby states increases.

and the low-l regime, $|E_{n,l}| \ll \Omega_0$ and $|l| \ll \sqrt{\delta/\Omega_0}$. Fig. 2(a) presents how this analytically found dispersion agrees with the numerical dispersion obtained by diagonalizing Eq. (2) (see Supplemental Material). As shown in the figure, the number of intragap state branches is given by $|m|$. The analytic dispersion and the numerical dispersion agree for the low-energy and low-l regime, and deviate from each other as the energy or l moves away from zero. Nevertheless, we can still use Eq. (4) to get a rough estimate of the pseudo-OAM differences between different intragap state branches, in the large optical vortex regime (see Supplemental Material). Assuming the entire intragap state branches are linearly dispersing, the different branches at the same energy would have the pseudo-OAM momentum difference of $\tilde{\omega}_0/\omega_0 = O\left(k_0 k_\delta^{-1}\sqrt{k_\delta\xi}\right)$. This large difference in the angular momentum prevents the vortex modes from different branches to hybridize each other. With the same assumption, the number of states in a single branch can be also estimated as $2\Omega_0/\omega_0 = O(k_0\xi)$.

Note that these Floquet vortex states around the optical vortex are distinguished from the edge states of topological Floquet Chern insulators [28] or the vortex states introduced in Ref. [30, 31]. For the edge state of the Floquet Chern insulator to develop, the bulk part of the system should have a non-zero Chern number, while the Floquet vortex states we are discussing appear regardless of the Chern number of the system. This point becomes clear by investigating the system under irradiation of a

circularly-polarized light beam which also carries a non-zero OAM (see Supplemental Material). While the bulk part of such system becomes a Floquet Chern insulator as explained in Ref. [28], there are still $|m|$ branches of Floquet vortex states in the middle of the hybridization gap. The Floquet vortex states in our system also differ from the vortex states in Ref. [30, 31] where the vortex structure does not couple with the electronic kinetic terms and has no trivial way to realize in experiments.

While many properties of the Floquet vortex states can be analyzed with the similar techniques used for superconducting vortex states, our Floquet vortex states have wider tunability due to the freedom to control the size of optical vortices. For superconducting vortex states, the size of vortices is tied to $O\left(k_\delta^{-1}\right)$ since the BdG equation should be satisfied in a self-consistent way. However, Eq. (2) does not have such constraints and we have the freedom to choose the size of the optical vortex. To illustrate the consequence of this freedom, we display the numerical dispersion for different optical vortex sizes in Fig. 2(b). As shown in the figure, as the optical vortex size ξ gets smaller, the linear region of the spectrum shrinks and therefore the non-linearity of the spectrum is enhanced. This adjustable non-linear dispersion of Floquet vortex states invites the possibility of using them as a platform for quantum state engineering.

IV. QUANTUM INFORMATION PROCESSING WITH FLOQUET VORTEX STATES

Since we can set shapes and locations of the optical vortices arbitrarily as well as can change them dynamically, the Floquet vortex states can be used to engineer and manipulate different quantum states with their wide range of tunability. To illustrate the potential utility of the Floquet vortex states as a platform for quantum state engineering, we show how one and two-qubit operations can be performed in this system. As we have seen in the previous section, we can increase the energy level spacing and the spectral non-linearity by reducing the size of the optical vortex. It is this enhanced non-linearity that allows to create qubits out of the Floquet vortex states and manipulate them (Fig. 3).

Specifically, we consider two Floquet vortex states with pseudo-angular momentum l_0 and $l_0 + 1$ of an intragap branch with index n. That is, $\langle\mathbf{r}|0\rangle \equiv \psi_{n,l_0}(\mathbf{r})$ and $\langle\mathbf{r}|1\rangle \equiv \psi_{n,l_0+1}(\mathbf{r})$. (While here we choose the vortex states from the same intragap branch, alternatively vortex states from different branches can be also used.) To manipulate this qubit, we may apply an extra linearly-polarized field to create an oscillating potential

$$V_{\text{ext}}(t) = e\mathcal{E}_{\text{ext}}\hat{\mathbf{n}}_{\mathbf{0}} \cdot \mathbf{r}\cos(\Omega_{\text{ext}}t), \tag{5}$$

where $\mathcal{E}_{\text{ext}}$ is the amplitude of the applied electric field and $\hat{\mathbf{n}}_{\mathbf{0}} = \cos\phi_0\hat{\mathbf{x}} + \sin\phi_0\hat{\mathbf{y}}$ is the polarization of the field. Then, in the rotating frame with frequency Ω_{ext},
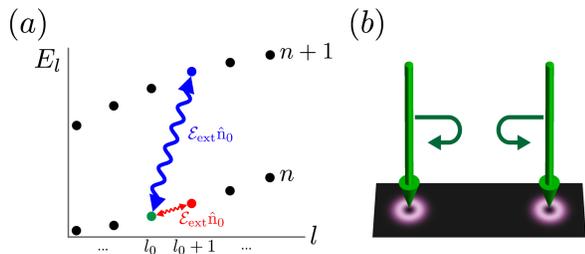
FIG. 3. (a) The non-linearity of the dispersion allows one to encode different Floquet vortex states as qubits. For example, the vortex states with pseudo-OAM l_0 and l_0+1 from the vortex state branch with index n (red arrow) or the branches with indices n and $n+1$ can be used to encode a qubit (blue arrow). Arbitrary single-qubit rotation can be performed by shining an extra linearly polarized light. While the polarization $\hat{\mathbf{n}}_0$ determines the rotation axis, the beam amplitude $\mathcal{E}_{\text{ext}}$ and the irradiation time determines the rotation angle. (b) Two-qubit gates can be performed by bringing two vortices close to each other and then separating them back.

the effective Hamiltonian for this qubit space becomes

$$H_{\text{1-qubit}} = \left(E_{l_0} + \frac{\Omega_{\text{ext}}}{2}\right)|0\rangle\langle 0| + \left(E_{l_0+1} - \frac{\Omega_{\text{ext}}}{2}\right)|1\rangle\langle 1|$$
$$+ \left[e\mathcal{E}_{\text{ext}}\langle 1|r\cos(\phi-\phi_0)|0\rangle|1\rangle\langle 0| + \text{H.c.}\right],$$

$$\langle 1|r\cos(\phi-\phi_0)|0\rangle = \int d^2\mathbf{r}\,\psi^\dagger_{n,l_0+1}(\mathbf{r})r\cos(\phi-\phi_0)\psi_{n,l_0}(\mathbf{r})$$

$$= \pi e^{i\phi_0}\sum_{s=\pm}\int_0^\infty u^*_{n,l_0+1,s}(r)u_{n,l_0,s}(r)r^2dr. \quad (6)$$

By setting $\Omega_{\text{ext}} = E_{n,l_0+1} - E_{n,l_0}$, we can effectively tune $H_{\text{1-qubit}}$ to be a superposition of σ_x and σ_y with an arbitrary ratio between them. Then this extra field implements an arbitrary single-qubit rotation where the rotation angle is tuned by the field amplitude $\mathcal{E}_{\text{ext}}$ and the irradiation time, while the rotational axis is set by the polarization $\hat{\mathbf{n}}_0$. Note that this qubit is isolated from other vortex states because the field with frequency matched to the energy difference $E_{n,l_0+1} - E_{n,l_0}$ cannot couple to other modes due to the non-linear dispersion of the vortex states (see Supplemental Material).

For two-qubit operations, we can move two vortices close to one another. This will lead to a hybridization, J, between the modes with the same quantum numbers on the two vortices. Yet, single-electron hopping from one vortex to another may be energetically unfavorable due to the on-site interaction energy U. This will generate an effective superexchange interaction $\sim J^2/U$, with the corresponding two-qubit Hamiltonian,

$$H_{\text{2-qubit}} = -\frac{J^2}{U}\left[|01\rangle\langle 01| + |10\rangle\langle 10| + (|10\rangle\langle 01| + \text{H.c.})\right], \quad (7)$$

where $|s_1 s_2\rangle = |s_1\rangle \otimes |s_2\rangle$ $(s_{1,2} = 0,1)$ are the computational basis for the two-qubit space. Since we have full control over the location of the vortices, we can tune our time-evolution operator to act as a $\sqrt{\text{SWAP}}$ gate up to

some single-qubit σ_z operations (see Supplemental Material). This $\sqrt{\text{SWAP}}$ gate and previously introduced single-qubit rotations constitute a gate set for universal quantum computation [49, 50]. We stress again that this proximity-based scheme of two-qubit gate is only possible because the current system allows enhanced freedom to change the locations of Floquet vortex states. This is a big advantage that Floquet vortex state qubits have over other qubits based on solid-state systems such as quantum dots [51–53].

While the state preparation in Floquet systems is a challenging problem in general, one may be able to prepare the desired Floquet state by using proper bosonic and fermionic reservoirs through dissipative engineering [34, 54, 55]. Once the initialization method is established, the desired qubit state can be prepared by controlling the backgate voltage, similar to the initialization procedure in quantum-dot qubit systems.

V. DISCUSSION AND OUTLOOK

The most important challenge in using periodic driving in condensed matter systems are the heating effects. However, recently there have been several theoretical proposals to restrain such destructive effects by using bath engineering techniques [34, 54–61]. In particular for Floquet topological insulators (FTI) [28] created by irradiating light to semiconductors as in our proposal, it has been demonstrated that in the weak-drive limit and in the presence of a phononic heat bath, heating effects produced by electron-electron and electron-phonon interactions can be suppressed provided that the bath-induced relaxation rates are sufficiently large [55]. For such baths key features of FTIs such as the existence of protected edge states can be preserved in the steady state which can make our proposal also stable in the steady state [62]. Also, recent experiments [36, 37] on the irradiated 2D material also provide another evidence that quantum states engineered by periodic driving on condensed matter systems can be stabilized in the lab.

While vortex states can also be engineered in cold atoms [8–12], there are several advantages to engineer them in electronic systems. One main advantage is the possibility of creating and manipulating multiple vortex states more conveniently, as demonstrated in the aforementioned qubit manipulation. While this is in principle possible in BEC systems too [63], controlling the transition of numerous atoms can be more challenging than manipulating a single electron. Also, our Floquet vortex state is spin-independent unlike the cold atom systems with spin-orbit-angular-momentum coupling [11, 12, 64–67], and this spin degrees of freedom can provide extra knobs for state engineering such as the Zeeman field.

To further elaborate the scheme for the quantum information processing, it would be interesting to study the possible measurement protocols for the OAM of the Floquet vortex states. One potential candidate for such

protocol is through the measurement of optical Hall conductivity, which might have different responses on the states with different OAM. Also, since our system has multiple non-linearly-dispersed Floquet vortex states, the extension to the qudit system is a natural topic for future study. While we briefly examined the possibility of such vortex state as a qubit, there are a lot of unanswered questions such as the heating, decoherence, and sensing in this platform. While we treated the vortex state of a single electron, it would be interesting to study how the presence of Coulomb interactions can change the vortex state structure or even help to create exotic many-body states. Another interesting direction is to investigate lattices of optical vortices and other field patterns such as electromagnetic skyrmions [68]. It would be also interesting to investigate how our approach can help to control optical properties of materials like van der Waals layered magnetic insulators [69].

[1] L. Onsager, Nuovo Cim **6**, 279 (1949).
[2] R. Feynman, Progress in Low Temperature Physics **1**, 17 (1955).
[3] A. A. Abrikosov, Sov. Phys. JETP **5**, 1174 (1957).
[4] C. Caroli, P. De Gennes, and J. Matricon, Physics Letters **9**, 307 (1964).
[5] R. Jackiw and P. Rossi, Nuclear Physics B **190**, 681 (1981).
[6] G. E. Volovik, The universe in a helium droplet, Vol. 117 (Oxford University Press on Demand, 2003).
[7] R. J. Donnelly, Quantized vortices in helium II, Vol. 2 (Cambridge University Press, 1991).
[8] M. R. Matthews, B. P. Anderson, P. C. Haljan, D. S. Hall, C. E. Wieman, and E. A. Cornell, Phys. Rev. Lett. **83**, 2498 (1999).
[9] K. W. Madison, F. Chevy, W. Wohlleben, and J. Dalibard, Phys. Rev. Lett. **84**, 806 (2000).
[10] J. R. Abo-Shaeer, C. Raman, J. M. Vogels, and W. Ketterle, Science **292**, 476 (2001).
[11] H.-R. Chen, K.-Y. Lin, P.-K. Chen, N.-C. Chiu, J.-B. Wang, C.-A. Chen, P. Huang, S.-K. Yip, Y. Kawaguchi, and Y.-J. Lin, Phys. Rev. Lett. **121**, 113204 (2018).
[12] D. Zhang, T. Gao, P. Zou, L. Kong, R. Li, X. Shen, X.-L. Chen, S.-G. Peng, M. Zhan, H. Pu, and K. Jiang, Phys. Rev. Lett. **122**, 110402 (2019).
[13] G. Blatter, M. V. Feigel'man, V. B. Geshkenbein, A. I. Larkin, and V. M. Vinokur, Rev. Mod. Phys. **66**, 1125 (1994).
[14] T. Maniv, V. Zhuravlev, I. Vagner, and P. Wyder, Rev. Mod. Phys. **73**, 867 (2001).
[15] A. Bogdanov and A. Hubert, Journal of Magnetism and Magnetic Materials **138**, 255 (1994).
[16] U. K. Roessler, A. Bogdanov, and C. Pfleiderer, Nature **442**, 797 (2006).
[17] N. Nagaosa and Y. Tokura, Nature nanotechnology **8**, 899 (2013).
[18] J. M. Kosterlitz and D. J. Thouless, Journal of Physics C: Solid State Physics **6**, 1181 (1973).
[19] J. M. Kosterlitz, Journal of Physics C: Solid State Physics **7**, 1046 (1974).
[20] P. A. Murthy, I. Boettcher, L. Bayha, M. Holzmann, D. Kedar, M. Neidig, M. G. Ries, A. N. Wenz, G. Zürn, and S. Jochim, Phys. Rev. Lett. **115**, 010401 (2015).

[21] D. S. Fisher, M. P. A. Fisher, and D. A. Huse, Phys. Rev. B **43**, 130 (1991).
[22] P. L. Gammel, L. F. Schneemeyer, J. V. Waszczak, and D. J. Bishop, Phys. Rev. Lett. **61**, 1666 (1988).
[23] R. H. Koch, V. Foglietti, W. J. Gallagher, G. Koren, A. Gupta, and M. P. A. Fisher, Phys. Rev. Lett. **63**, 1511 (1989).
[24] C. Nayak, S. H. Simon, A. Stern, M. Freedman, and S. Das Sarma, Rev. Mod. Phys. **80**, 1083 (2008).
[25] M. Stone and S.-B. Chung, Phys. Rev. B **73**, 014505 (2006).
[26] K. T. Kapale and J. P. Dowling, Phys. Rev. Lett. **95**, 173601 (2005).
[27] T. Oka and H. Aoki, Phys. Rev. B **79**, 081406(R) (2009).
[28] N. H. Lindner, G. Refael, and V. Galitski, Nature Physics **7**, 490 (2011).
[29] M. C. Rechtsman, J. M. Zeuner, Y. Plotnik, Y. Lumer, D. Podolsky, F. Dreisow, S. Nolte, M. Segev, and A. Szameit, Nature **496**, 196 (2013).
[30] Y. T. Katan and D. Podolsky, Phys. Rev. Lett. **110**, 016802 (2013).
[31] Y. Tenenbaum Katan and D. Podolsky, Phys. Rev. B **88**, 224106 (2013).
[32] N. Goldman and J. Dalibard, Phys. Rev. X **4**, 031027 (2014).
[33] P. Titum, E. Berg, M. S. Rudner, G. Refael, and N. H. Lindner, Phys. Rev. X **6**, 021013 (2016).
[34] H. Dehghani, T. Oka, and A. Mitra, Phys. Rev. B **90**, 195429 (2014).
[35] H. Kim, H. Dehghani, H. Aoki, I. Martin, and M. Hafezi, Phys. Rev. Research **2**, 043004 (2020).
[36] J. W. McIver, B. Schulte, F. U. Stein, T. Matsuyama, G. Jotzu, G. Meier, and A. Cavalleri, Nature Physics **16**, 38 (2020).
[37] S. A. Sato, J. W. McIver, M. Nuske, P. Tang, G. Jotzu, B. Schulte, H. Hübener, U. De Giovannini, L. Mathey, M. A. Sentef, A. Cavalleri, and A. Rubio, Phys. Rev. B **99**, 214302 (2019).
[38] P. Zupancic, P. M. Preiss, R. Ma, A. Lukin, M. E. Tai, M. Rispoli, R. Islam, and M. Greiner, Opt. Express **24**, 13881 (2016).
[39] D. Barredo, S. de Léséleuc, V. Lienhard, T. Lahaye, and A. Browaeys, Science **354**, 1021 (2016).

[40] D. Barredo, V. Lienhard, S. De Leseleuc, T. Lahaye, and A. Browaeys, Nature **561**, 79 (2018).

[41] N. Schine, M. Chalupnik, T. Can, A. Gromov, and J. Simon, Nature **565**, 173 (2019).

[42] B. A. Bernevig, T. L. Hughes, and S.-C. Zhang, Science **314**, 1757 (2006).

[43] E. G. Novik, A. Pfeuffer-Jeschke, T. Jungwirth, V. Latussek, C. R. Becker, G. Landwehr, H. Buhmann, and L. W. Molenkamp, Phys. Rev. B **72**, 035321 (2005).

[44] G. Volovik, JETP Lett. **57**, 244 (1993).

[45] C. Caroli, P. De Gennes, and J. Matricon, Physics Letters **9**, 307 (1964).

[46] Y. Tada, W. Nie, and M. Oshikawa, Phys. Rev. Lett. **114**, 195301 (2015).

[47] T. Ojanen, Phys. Rev. B **93**, 174505 (2016).

[48] A. Prem, S. Moroz, V. Gurarie, and L. Radzihovsky, Phys. Rev. Lett. **119**, 067003 (2017).

[49] D. P. DiVincenzo, D. Bacon, J. Kempe, G. Burkard, and K. B. Whaley, Nature **408**, 339 (2000).

[50] H. Fan, V. Roychowdhury, and T. Szkopek, Phys. Rev. A **72**, 052323 (2005).

[51] D. Loss and D. P. DiVincenzo, Phys. Rev. A **57**, 120 (1998).

[52] B. E. Kane, nature **393**, 133 (1998).

[53] R. Vrijen, E. Yablonovitch, K. Wang, H. W. Jiang, A. Balandin, V. Roychowdhury, T. Mor, and D. DiVincenzo, Phys. Rev. A **62**, 012306 (2000).

[54] I. Esin, M. S. Rudner, G. Refael, and N. H. Lindner, Phys. Rev. B **97**, 245401 (2018).

[55] K. I. Seetharam, C.-E. Bardyn, N. H. Lindner, M. S. Rudner, and G. Refael, Phys. Rev. B **99**, 014307 (2019).

[56] H. Dehghani, T. Oka, and A. Mitra, Phys. Rev. B **91**, 155422 (2015).

[57] T. Iadecola and C. Chamon, Phys. Rev. B **91**, 184301 (2015).

[58] T. Shirai, T. Mori, and S. Miyashita, Phys. Rev. E **91**, 030101(R) (2015).

[59] H. Dehghani and A. Mitra, Phys. Rev. B **92**, 165111 (2015).

[60] H. Dehghani and A. Mitra, Phys. Rev. B **93**, 245416 (2016).

[61] T. Kuwahara, T. Mori, and K. Saito, Annals of Physics **367**, 96 (2016).

[62] Since the additional number of vortex states in our system compared to FTIs, is finite we expect the results obtained in [55] should be applicable to our system, too.

[63] M. F. Andersen, C. Ryu, P. Cladé, V. Natarajan, A. Vaziri, K. Helmerson, and W. D. Phillips, Phys. Rev. Lett. **97**, 170406 (2006).

[64] M. DeMarco and H. Pu, Phys. Rev. A **91**, 033630 (2015).

[65] K. Sun, C. Qu, and C. Zhang, Phys. Rev. A **91**, 063627 (2015).

[66] K.-J. Chen, F. Wu, S.-G. Peng, W. Yi, and L. He, Phys. Rev. Lett. **125**, 260407 (2020).

[67] L.-L. Wang, A.-C. Ji, Q. Sun, and J. Li, Phys. Rev. Lett. **126**, 193401 (2021).

[68] S. Tsesses, E. Ostrovsky, K. Cohen, B. Gjonaj, N. Lindner, and G. Bartal, Science **361**, 993 (2018).

[69] D. Hsieh, Private Communication (2021).